

# Cryptoferromagnetism in Superconductors with Broken Time-Reversal-Symmetry

N. A. Logoboy and E. B. Sonin

*Racah Institute of Physics, The Hebrew University of Jerusalem, Jerusalem 91904, Israel*

(Dated: August 11, 2021)

The cryptoferromagnetic state (the state with intrinsic domain structure) in superconducting ferromagnets subjected to external magnetic field is studied theoretically. Ferromagnetism originates either from electron spin or the intrinsic angular momentum of Cooper pairs (chiral  $p$ -wave superconductors like  $\text{Sr}_2\text{RuO}_4$ ). The phase transitions towards the Meissner and the mixed states are investigated, and the magnetic phase diagrams are obtained. Cryptoferromagnetism, as a form coexistence of superconductivity and ferromagnetism, can be detected by observation of magnetization curves predicted in the present analysis.

PACS numbers: 74.25.Ha, 74.90.+n, 75.60.-d

In recent years numerous experimental evidences of superconductivity-ferromagnetism coexistence in various materials were reported [1, 2, 3, 4, 5, 6]. Two types of such coexistence are possible: (i) The phase transitions to the ferromagnetic and the superconducting (SC) states occurs at different temperatures, so the coexistence starts below the lower from the two transitions. Ruthenocuprates [1] belong to this type: the superconductivity onset occurs at the temperature much lower than the temperature of the magnetic transition. Normally different elements of the crystal structure are responsible for ferromagnetism and superconductivity, and spontaneous magnetization (ferromagnetic order parameter) is related to spin. Later we call them spin superconducting ferromagnets (spin SFs). (ii) The magnetic and the SC transitions occur simultaneously. This can take place in unconventional superconductors with triplet Cooper pairing. An example of them is strontium ruthenate  $\text{Sr}_2\text{RuO}_4$  [3, 4, 7]. The theory connects spontaneous magnetization in this material not with spin but with the orbital intrinsic angular moment of the  $p$ -wave Cooper pair with the wave function in the momentum space proportional to  $p_x + ip_y$  (chiral  $p$ -wave superconductivity). We shall call them orbital superconducting ferromagnets (orbital SFs).

Whereas proof of superconductivity in SF materials is quite straightforward, a clear-cut detection of the ferromagnetic order parameter is much more problematic. The internal magnetic field is screened out by the SC Meissner currents and can be present only near sample borders and defects, in particular, domain walls (DWs). This strongly suppresses the stray magnetic fields around the sample, which are most convincing evidence of ferromagnetism. Especially worrying is situation with strontium ruthenate  $\text{Sr}_2\text{RuO}_4$ , where Kirtley *et al.* [8] could not detect any stray field from DWs or sample edges at all. This is a challenge for the theory and for the very scenario of chiral  $p$ -wave pairing. Difficulties with direct detection of ferromagnetism coexisting with superconductivity lead to the question whether one may use the term *ferromagnetism* at all. Indeed in the literature on unconventional superconductors sometimes they prefer to tell about *superconductivity with broken Time-Reversal Sym-*

*metry* (TRS). We used this name in the title of the paper following this more cautious semantics though one cannot imagine broken TRS without at least some features of ferromagnetism (see further discussion).

Among possible explanations why experimentalists cannot see stray fields from DWs is the presence of domain structure with a period essentially smaller than a distance between a sample surface and a probe used by experimentalists. There were some experimental evidences of domains in SFs both in the spin [9] and the orbital SF [10]. The theoretical investigations of the domain structure in SFs were restricted with the case of zero external magnetic field [11, 12, 13, 14]. One must discern two possible types of equilibrium domain structure. The first one is well known for normal ferromagnets [15]. The domain structure results from competition between the energy of DWs and the magnetostatic energy of stray fields generated by the magnetic flux exiting from the sample surface. The period of the structure depends on the shape and the size of the sample going to infinity when the sample size grows. One can call these domains *extrinsic ferromagnetic domains*. Since in SFs the Meissner effect expels the magnetic field, it is impossible to benefit from decreasing the bulk magnetostatic energy in comparison with the DW energy, and extrinsic domains cannot appear at equilibrium [12]. But also long ago there was known another type of domains, which decrease the bulk magnetostatic energy at the expense of destroying the Meissner state [11, 13, 14]. The size of these domains is roughly of the order of the London penetration depth  $\lambda$  and does not depend on either shape or size of the sample. Strictly speaking the state with this domain structure at the macroscopic scales is not ferromagnetic but antiferromagnetic though with a rather large period. We shall call such a state *cryptoferromagnetic*, the term introduced by Anderson and Suhl [16] for another model of ferromagnetism and superconductivity, in which crystal anisotropy was neglected and spiral structure appeared instead of domains.

In present publication we extend the theory of intrinsic domain structure (cryptoferromagnetic state) on nonzero external magnetic field and analyze competition of the cryptoferromagnetic state with the pure Meissner state

and the mixed state with vortices. This allows to obtain the full phase diagram of both spin and orbital SFs. We demonstrate that the measurement of magnetization curves in various areas of the phase diagram can provide evidence of ferromagnetic or cryptoferromagnetic order in superconductors with broken TRS.

Let us consider a stripe domain structure with  $180^\circ$  DWs in a sample subjected to external magnetic field  $\mathbf{H}_0 = (0, H_0, 0)$ . The DWs are parallel to the  $yz$ -plane separating domains with alternating magnetization  $\mathbf{M} = (0, \pm M_0, 0)$  along the  $+y$  or  $-y$  direction. Since the  $\mathbf{H}_0$  orientation is preferable the width  $d_\uparrow$  of domains with the magnetization  $\mathbf{M}$  parallel to  $\mathbf{H}_0$  ( $\uparrow$ -domains) exceeds the width  $d_\downarrow$  of the domains with  $\mathbf{M}$  antiparallel to  $\mathbf{H}_0$  ( $\downarrow$ -domains). We restrict ourselves to the simplest case when the London penetration length  $\lambda$  exceeds the DW thickness. Then the surface energy  $\sigma$  and the internal structure of DW is not affected by fields and currents at scales of  $\lambda$ .

The Gibbs potential inside domains is

$$\mathcal{G} = \int d^3x \left( \frac{\mathbf{h}^2}{8\pi} + \frac{2\pi\lambda^2}{c^2} \mathbf{j}^2 - \mathbf{h} \cdot \mathbf{M} - \frac{\mathbf{h} \cdot \mathbf{H}_0}{4\pi} \right), \quad (1)$$

where  $\mathbf{h}$  is the magnetic field, and the electric current  $\mathbf{j}$  is connected with the magnetic field  $\mathbf{h}$  via the Maxwell equation  $\nabla \times \mathbf{h} = (4\pi/c)\mathbf{j}$ . Variation of the Gibbs potential yields the magnetic field  $\mathbf{h}_{\uparrow,\downarrow} = (0, h_{\uparrow,\downarrow}, 0)$  in the  $\uparrow$ -domains and  $\downarrow$ -domains:

$$h_{\uparrow,\downarrow} = (H_0 \pm 4\pi M_0) \frac{\cosh(x/\lambda - \xi_{\uparrow,\downarrow})}{\cosh \xi_{\uparrow,\downarrow}}, \quad (2)$$

where  $x$  is the distance from the DW and  $\xi_{\uparrow,\downarrow} = d_{\uparrow,\downarrow}/2\lambda$  are reduced domain widths.

Application of the Gibbs potential Eq. (1) to orbital SFs requires some comments. As shown in Ref. [17], for orbital ferromagnetism related to the intrinsic angular momentum of Cooper pairs the spontaneous magnetization cannot be defined unambiguously and therefore the Landau-Lifshitz theory of ferromagnetism [15] based on this definition is not valid. Nevertheless, interaction of magnetization currents inside narrow DW with the magnetic field can be reduced to the expression looking like the standard Zeeman energy  $-\mathbf{h} \cdot \mathbf{M}_0$ . However, here  $\mathbf{M}_0$  is not a magnetic moment inside the domain but is defined so that  $8\pi M_0$  would be the jump  $8\pi M_0$  of the magnetic field on the DW [see Eq. (2)]. So ‘‘magnetization’’  $M_0$  is determined by the DW structure and cannot be used for other phenomena connected with ferromagnetic ordering, e.g., analyzing the magnon spectrum [17].

Substituting Eq. (2) into Eq. (1), adding the surface energy  $\sigma$  of DWs, and averaging over the domain-structure period  $d = d_\uparrow + d_\downarrow$  we arrive to the following expression for reduced energy density  $\mathcal{E} = \mathcal{G}/2\pi M_0^2 V$  ( $V$  is the sample volume):

$$\mathcal{E} = \frac{2w - (1 + h_0)^2 \tanh \xi_\uparrow - (1 - h_0)^2 \tanh \xi_\downarrow}{\xi_\uparrow + \xi_\downarrow}. \quad (3)$$

Here  $h_0 = H_0/4\pi M_0$  and  $w = \sigma/4\pi M_0^2 \lambda$  are dimensionless parameters. If  $h_0 = 0$  and  $\xi_\uparrow = \xi_\downarrow$  Eq. (3) coincides with the free energy density of Krey [11].

Minimization of energy density Eq. (3) with respect to  $\xi_\uparrow$  and  $\xi_\downarrow$  yields the system of two nonlinear equations for  $\xi_\uparrow$  and  $\xi_\downarrow$ :

$$\begin{aligned} \tanh \frac{\xi_\uparrow - \xi_\downarrow}{2} \tanh \frac{\xi_\uparrow + \xi_\downarrow}{2} &= h_0, \\ \frac{\sinh 2\xi_\uparrow + \sinh 2\xi_\downarrow - 2(\xi_\uparrow + \xi_\downarrow)}{(\cosh \xi_\uparrow + \cosh \xi_\downarrow)^2} &= w. \end{aligned} \quad (4)$$

The magnetic induction  $\mathbf{B} = \langle \mathbf{h} \rangle$  is determined by reduced magnetic induction  $b = B/4\pi M_0$ :

$$b = -\frac{1}{2} \frac{\partial \mathcal{E}}{\partial h_0} = \frac{(1 + h_0) \tanh \xi_\uparrow - (1 - h_0) \tanh \xi_\downarrow}{\xi_\uparrow + \xi_\downarrow}. \quad (5)$$

Fig. 1(a) shows the phase diagram in the plane  $w^2 - h_0$ . The area of the cryptoferromagnetic state is restricted by two lines where the phase transition between the cryptoferromagnetic and the Meissner states occurs:

1. The line  $\mathcal{E} = 0$ , which corresponds to the limit  $\xi_{\uparrow,\downarrow} \rightarrow \infty$ . The values of  $w$  and  $h_0$  on this line are connected by the relation  $w = 1 + h_0^2$ .

2. The line on which domains with magnetization opposite to the external magnetic field vanish,  $\xi_\downarrow = 0$ . The equation describing this line is

$$w_c = \sqrt{h_c}(1 + h_c) - \frac{(1 - h_c)^2}{2} \ln \frac{1 + \sqrt{h_c}}{1 - \sqrt{h_c}}, \quad (6)$$

the critical size of the  $\uparrow$ -domain being

$$\xi_{\uparrow c} = \ln \frac{1 + \sqrt{h_c}}{1 - \sqrt{h_c}}. \quad (7)$$

The magnetic induction on the critical line is

$$b_c = 2\sqrt{h_c} \left( \ln \frac{1 + \sqrt{h_c}}{1 - \sqrt{h_c}} \right)^{-1}. \quad (8)$$

Let us consider the left lower corner of this diagram where  $w \ll 1$  and  $h_0 \ll 1$ . The critical parameters on the line  $\xi_\downarrow = 0$  as functions of  $w$  are

$$h_c = \frac{1}{4}(3w)^{2/3}, \quad \xi_{\uparrow c} = (3w)^{1/3}. \quad (9)$$

Aside from the critical line Eqs. (4) yield:

$$h_0 = \frac{\xi_\uparrow^2 - \xi_\downarrow^2}{4}, \quad w = \frac{\xi_\uparrow^3 + \xi_\downarrow^3}{3}. \quad (10)$$

For small  $h_0 \ll h_c$  one can solve Eqs. (10) analytically:

$$\xi_{\uparrow,\downarrow} = 4^{1/3} \sqrt{h_c} \left( 1 - \frac{h_0^2}{4^{4/3} h_c^2} \right) \pm \frac{h_0}{4^{1/3} \sqrt{h_c}}. \quad (11)$$

Let us consider the magnetization curve in the cryptoferromagnetic state. The linear magnetic permeability is

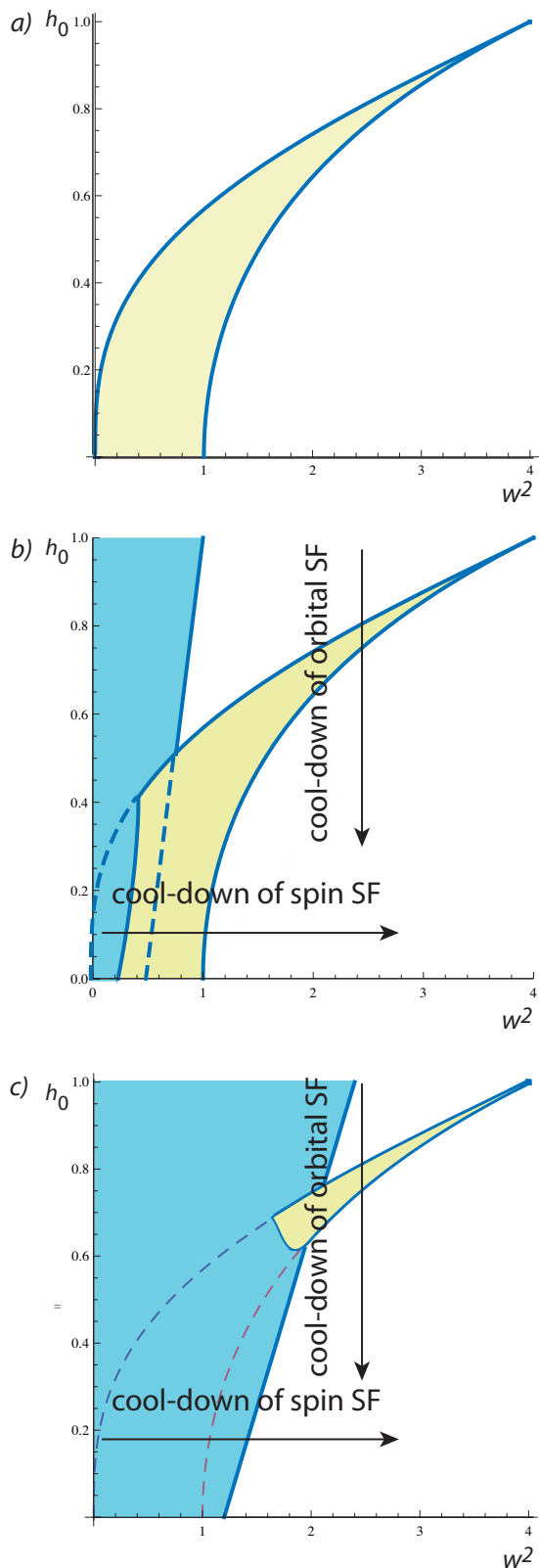


FIG. 1: (color online) Phase diagram for various values of the reduced lower critical field  $h_{c1}$ : (a)  $h_{c1} \rightarrow \infty$ ; (b)  $h_{c1} = 2$ ; (c)  $h_{c1} = 0.83$ . The lighter (yellow) shaded area is the cryptoferromagnetic state. The darker (blue) shaded area is the mixed state. The rest is the Meissner state. The horizontal and the vertical arrows show the processes of cool-down across the SC critical temperature of spin and orbital SFs respectively.

determined from two relations connecting  $\mu$  and  $w$  with the period  $\xi = \xi_{\uparrow} + \xi_{\downarrow} \approx 2\xi_{\uparrow}$

$$\mu = \frac{db}{dh_0} = \frac{\coth \xi}{\xi}, \quad w = \tanh \xi - \frac{\xi}{\cosh \xi}. \quad (12)$$

In the limit  $w \rightarrow 0$  the magnetic permeability is divergent:  $\mu \approx (2/3w)^{2/3}$ . The whole magnetization curves  $b(h_0)$ , which were calculated numerically, are shown in Fig. 2(a).

Fig. 2(b) shows the dependence of the period  $\xi = \xi_{\uparrow} + \xi_{\downarrow}$  and the difference of the two domain widths  $\delta = \xi_{\uparrow} - \xi_{\downarrow}$  as functions of the reduced external magnetic field  $h_0$ .

Up to now we ignored the possibility of the transition to the mixed state assuming that the first critical magnetic field  $H_{c1} = \Phi_0 \ln \kappa / 4\pi \lambda^2$  essentially exceeds the characteristic fields of the cryptoferromagnetic state. Here  $\kappa = \lambda / \xi_0$  is the ratio of  $\lambda$  to the coherence length  $\xi_0$ . Let us now take into account this possibility. Both the field  $H_{c1}$  and the parameter  $w$  depend on the penetration depth  $\lambda$ , and it is useful to introduce the reduced first critical field  $h_{c1} = H_{c1} / 4\pi M_0 w^2 = \Phi_0 M_0^3 \ln \kappa / \sigma^2$ , which does not depend on  $\lambda$ . The reduced free energy of the mixed state with respect to the energy of the Meissner state is

$$\mathcal{E}_m = - \left( 1 + h_0 - \frac{H^*}{4\pi M} \right)^2 = - (1 + h_0 - h_{c1} w^2)^2, \quad (13)$$

where the field  $H^*$  inside the mixed state differs from  $H_{c1}$  by another logarithm factor, but we neglect it assuming  $H^* \approx H_{c1}$ . The phase transition to the mixed state may occur either from the Meissner state being determined by the condition  $\mathcal{E}_m = 0$ , or from the cryptoferromagnetic state crossing the critical line on which  $\mathcal{E}_m = \mathcal{E}$ . At zero external field  $h_0$  and small  $w$  the phase transition between the mixed state and the cryptoferromagnetic state occurs at  $w_m \approx \sqrt{3}/(2h_{c1})^{3/4}$ . Thus whatever large  $h_{c1}$  is, in the left lower corner of the phase diagram there is always *the spontaneous vortex phase*, i.e., the mixed state without external magnetic field. The full phase diagrams at two finite values  $h_{c1} = 2$  and  $0.83$  are shown in Figs. 1(b) and (c). The cryptoferromagnetic state disappears from the phase diagram at  $h_{c1} < 0.5$ .

Now let us analyze the phase transformations in the process of cooling down below the SC critical temperature. This process is different for spin and orbital SFs. In the case of spin SFs, when the magnetic transition occurs at much higher temperature, one may neglect temperature dependence of  $M_0$ ,  $\sigma$ , and  $h_{c1}$ . Then only  $w^2 \propto 1/\lambda^2 \propto \tau$  depends on relative temperature difference  $\tau = (T_c - T)/T_c$ . On the phase diagrams of Figs. 1(b) and (c) the state moves along straight lines parallel to the horizontal axis  $w^2$ . From these figures it is evident that just below the critical temperature the system enters the mixed state. At further cooling down the system crosses to the Meissner state either directly or through the area of the cryptoferromagnetic state. For orbital SFs the cooling process occurs differently. In

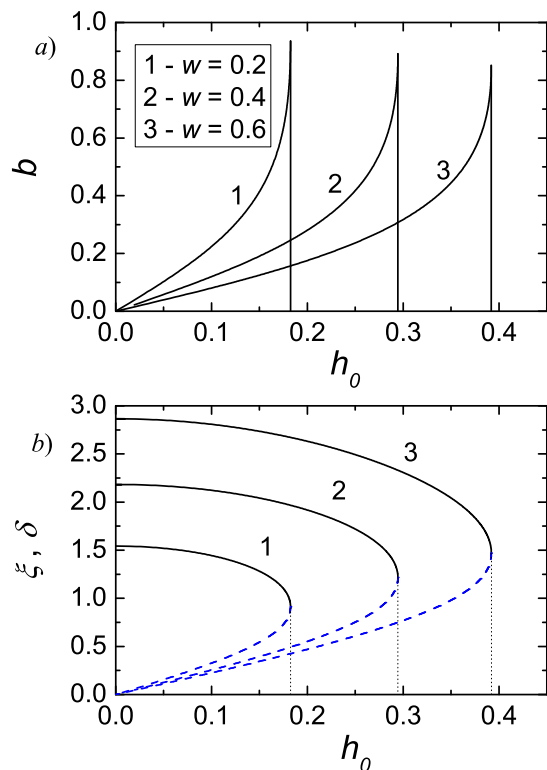


FIG. 2: (color online) (a) Magnetization curves and (b) magnetic field dependencies of  $\xi = \xi(h_0)$  (solid line) and  $\delta = \delta(h_0)$  (dash line) are shown at different values of parameter  $w$ . Vertical lines correspond to critical fields above which the intrinsic domain structure collapses.

this case the “magnetization”  $M_0 \sim \Phi/\lambda^2 \propto \tau$ , and the

DW surface energy is a product of the condensation energy  $H_c^2(\tau) \sim [\Phi_0/\lambda(\tau)\xi_0(\tau)]^2$  and the coherence length  $\xi_0(\tau) \sim \xi_0/\sqrt{\tau}$ :  $\sigma \sim \tau^{3/2}\Phi_0^2/\lambda_0^2\xi_0$ . Here  $\lambda_0$  and  $\xi_0$  are the penetration depth and the coherence length at zero temperature. Then the parameters  $w^2 \sim h_{c1}^{-1} \sim (\lambda_0/\xi_0)^2$  do not depend on temperature whereas the reduced magnetic field does:  $h_0 = H_0/4\pi M_0 \propto 1/\tau$ . Thus in the field-cooling process the state moves along vertical lines on the phase diagrams in Figs. 1(b) and (c). However, as pointed out above, the cryptoferromagnetic state can compete with the mixed state only if  $h_{c1}$  is high enough. Since  $h_{c1} \sim (\xi_0/\lambda_0)^2$ , this requires  $\lambda_0$  not large compared to  $\xi_0$ . According to [8] the ratio of  $\lambda_0 = 190$  nm to  $\xi_0 = 66$  nm is not too high indeed. But this means that the DW thickness is not so small compared to  $\lambda$  as assumed in our analysis. Therefore for orbital SFs our analysis can provide only a qualitative but still credible picture of the phase transformations.

In conclusion, we analyzed the conditions for appearance of intrinsic domains in superconductors with broken time reversal symmetry, in which superconductivity coexists either with spin ferromagnetism or with ferromagnetism originated from the intrinsic angular momentum of Cooper pairs (chiral  $p$ -wave superconductors like  $\text{Sr}_2\text{RuO}_4$ ). Since these domains strictly speaking correspond not to a ferromagnetic but a globally antiferromagnetic state, the state was called *cryptoferromagnetic*. We considered competition of this state with the Meissner and the mixed states and found the phase diagram. This phase diagram can be checked with detailed measurements of magnetization curves.

This work has been supported by the grant of the Israel Academy of Sciences and Humanities.

- 
- [1] I. Felner, U. Asaf, Y. Levi, and O. Milo, Phys. Rev. B **55**, 3374 (1997).  
[2] M. R. Eskildsen, K. Harada, P. L. Gammel, A. B. Abrahamsen, N. H. Andersen, G. Ernst, A. P. Ramirez, D. J. Bishop, K. Mortensen, D. G. Naugle, K. D. D. Rathnayaka, and P. C. Canfield, Nature (London) **393**, 242 (1998).  
[3] G. M. Luke, Y. Fudamoto, K. M. Kojima, M. I. Larkin, J. Merrin, B. Nachumi, Y. J. Uemura, Y. Maeno, Z. Q. Mao, Y. Mori, H. Nakamura and M. Sigrist, Nature (London) **394**, 558 (1998).  
[4] K. Ishida, H. Mukuda, Y. Kitaoka, K. Asayama, Z. Q. Mao, Y. Mori, and Y. Maeno, Nature (London) **396**, 658 (1998).  
[5] S. S. Saxena, P. Agarwal, K. Ahilan, F. M. Grosche, R. K. W. Haselwimmer, M. J. Steiner, E. Pugh, I. R. Walker, S. R. Julian, P. Monthoux, G. G. Lonzarich, A. Huxley, I. Sheikin, D. Braithwaite, and J. Flouquet, Nature (London) **406**, 587 (2000).  
[6] C. Pfeleiderer, M. Uhlarz, S. M. Hayden, R. Vollmer, H. v. Löhneysen, N. R. Bernhoeft, and G. G. Lonzarich, Nature (London) **412**, 58 (2001).  
[7] A. P. Mackenzie and Y. Maeno, Rev. Mod. Phys. **75**, 657 (2003).  
[8] J. R. Kirtley, C. Kallin, C. W. Hicks, E.-A. Kim, Y. Liu, K. A. Moler, Y. Maeno, and K. D. Nelson, Phys. Rev. B **76**, 014526 (2007).  
[9] G. I. Leviev, M. I. Tsindlekht, E. B. Sonin, and I. Felner, Phys. Rev. B **70**, 212503 (2004).  
[10] F. Kidwingira, J. D. Strand, D. J. Van Harlingen, and Y. Maeno, Science, **314** (2006).  
[11] U. Krey, Intern. J. Magn. **3**, 65 (1972).  
[12] E. B. Sonin, Phys. Rev. B **66**, 100504(R) (2002).  
[13] M. Fauré and A. I. Buzdin, Phys. Rev. Lett. **94**, 187202 (2005).  
[14] E. B. Sonin, Phys. Rev. Lett. **95**, 269701 (2005); M. Fauré and A. I. Buzdin, Phys. Rev. Lett. **95**, 269702 (2005).  
[15] L.D. Landau and E.M. Lifshitz, *Electrodynamics of Continuous Media* (Pergamon Press, Oxford, 1984).  
[16] P. W. Anderson and H. Suhl, Phys. Rev. **116** 898 (1959).  
[17] V. Braude and E. B. Sonin, Phys. Rev. B **74**, 064501 (2006).